

# Influence of vesicle surface composition on the interfacial binding of lecithin:cholesterol acyltransferase and apolipoprotein A-I

Katherine R. Miller and John S. Parks<sup>1</sup>

Department of Comparative Medicine, The Bowman Gray School of Medicine of Wake Forest University, Medical Center Boulevard, Winston-Salem, NC 27157

**Abstract** Interfacial binding affinities and capacities of lecithin:cholesterol acyltransferase (LCAT) and apolipoprotein A-I (apoA-I) for surfaces of different phosphatidylcholine (PC) composition, cholesterol content, and apolipoprotein content were measured with a vesicle model system. Native polyacrylamide gel electrophoresis was used to separate free protein from vesicle-bound protein. ApoA-I was isolated from human plasma and radiolabeled with iodine, whereas radiolabeled LCAT was purified from the media of Chinese hamster ovary cells that were transfected with human LCAT cDNA and incubated in the presence of [<sup>35</sup>S] cysteine and methionine. Bound and free radiolabeled LCAT and apoA-I were quantified by phosphorimage analysis. ApoA-I binding was not influenced by cholesterol content (14 mole%) but was influenced by the PC fatty acyl composition of the vesicle. PC species containing long chain, polyunsaturated fatty acids (PUFA) in the *sn*-2 position resulted in increased binding affinity ( $K_d = 75\text{--}177\text{ nm}$ ) but reduced capacity (0.1–0.3 apoA-I/1000 PC) in comparison to *sn*-1 palmitoyl, *sn*-2 oleoyl PC (POPC, 750 nm and 1.4 apoA-I/1000 PC). LCAT binding affinity to POPC (2190 nm) was stronger in the presence of cholesterol (530 nm), and LCAT binding capacity was reduced (2.63 and 0.6 molecules LCAT/1000 PC, respectively). In comparison to POPC, LCAT binding affinity to *sn*-1 palmitoyl, *sn*-2 arachidonoyl PC was stronger (611 nm) and binding capacity was reduced (0.7 LCAT/1000 PC). LCAT binding affinity and capacity to *sn*-1 palmitoyl, *sn*-2 eicosapentaneoyl PC (2041 nm, and 2.5 LCAT/1000 PC) were similar to those observed for POPC. We conclude that vesicle surface PC fatty acyl composition and cholesterol content significantly influence LCAT and apoA-I interfacial binding and therefore may alter LCAT enzymatic activity.—Miller, K. R., and J. S. Parks. Influence of vesicle surface composition on the interfacial binding of lecithin:cholesterol acyltransferase and apolipoprotein A-I. *J. Lipid Res.* 1997. **38**: 1094–1102.

**Supplementary key words** gel electrophoresis • polyunsaturated fatty acids • binding affinity • binding capacity • phosphatidylcholine • cholesterol

The maturation of nascent, discoidal high density lipoproteins (HDL) is the result of cholesteryl ester formation by lecithin:cholesterol acyltransferase (LCAT)

from HDL phospholipid and cholesterol. In order to function, LCAT, a soluble plasma enzyme, must bind to the lipid/water interface of the HDL particle and be activated by apolipoprotein A-I (apoA-I), the main structural protein of HDL. Interfacial binding of LCAT may be mediated by a putative amphipathic helix in the region of residues 150–175 (1, 2). LCAT also contains a hexapeptide active site motif (residues 178–183) that is homologous to that in other lipases including pancreatic lipase, lipoprotein lipase, and hepatic lipase (1, 3–5).

The phospholipid fatty acyl composition of HDL has a strong influence on LCAT activity. For instance, LCAT activity on recombinant HDL (rHDL) demonstrated reduced  $V_{max}$  for particles synthesized from phospholipids containing long chain, polyunsaturated fatty acids (PUFA) in the *sn*-2 position compared to rHDL containing POPC (6–9). The  $K_m$  also varied 2-fold with the phospholipid composition. However, few direct measurements of LCAT interfacial binding have been reported. Bolin and Jonas (10) developed solid phase and activity inhibition assays for the measurement of LCAT binding to rHDL particles. Dissociation constants of 17–27  $\mu\text{M}$  PC for the two assays were determined for rHDL consisting of egg yolk PC, free cholesterol, and apoA-I. In another study Bolin and Jonas (11) examined the effect of rHDL sphingomyelin content on LCAT binding. Using the activity inhibition assay, dissociation constants for LCAT binding to rHDL containing egg yolk PC ranged from 23  $\mu\text{M}$  PC to 69  $\mu\text{M}$  PC in the

Abbreviations: LCAT, lecithin:cholesterol acyltransferase; POPC, *sn*-1 palmitoyl, *sn*-2 oleoyl phosphatidylcholine; PAPC, *sn*-1 palmitoyl, *sn*-2 arachidonoyl phosphatidylcholine; PEPC, *sn*-1 palmitoyl, *sn*-2 eicosapentaneoyl phosphatidylcholine; PDPC, *sn*-1 palmitoyl, *sn*-2 docosahexaenoyl phosphatidylcholine; HDL, high density lipoprotein; PC, phosphatidylcholine; apoA-I, apolipoprotein A-I.

<sup>1</sup>To whom correspondence should be addressed.

absence and presence of 22 mole% sphingomyelin, respectively. Weinberg et al. (12) measured LCAT binding using a monolayer system and found a dissociation constant of 1.5 nM LCAT with egg yolk PC monolayers.

In contrast to LCAT, apoA-I binding to phospholipids has been more extensively examined. ApoA-I binding affinities have been measured using lipid monolayers (13), vesicles (14), and lipid emulsions (15). However, only one study has examined the influence of PUFA in PC on apoA-I binding (13). In that study, the authors concluded that PC containing PUFA decreased apoA-I binding affinity and capacity for the monolayer surface. ApoA-I binding studies as a function of PC fatty acyl composition using model systems other than the monolayer have not been performed.

The purpose of the present study was to quantify the influence of phospholipid surface composition on LCAT and apoA-I interfacial binding using a vesicle model system. Vesicles were chosen because their size and shape can be well controlled, and they have a spherical shape like mature lipoproteins. A native polyacrylamide gel system was developed to measure apoA-I and LCAT binding affinities and capacities to PC species with different fatty acyl groups in the *sn*-2 position. The influences of apoA-I and cholesterol on LCAT binding were also examined. From these results, we conclude that surface lipid composition influences LCAT and apoA-I interfacial binding affinities and capacities. Cholesterol further modulates LCAT binding and may play a significant role in determining the affinity and capacity of the enzyme for the interface of HDL.

## METHODS

### <sup>35</sup>S-labeled LCAT expression and purification

Chinese hamster ovary cells (CHO) that were stably transfected with pCMV-5 human LCAT cDNA (16) were grown to ~50% confluence in DMEM/Coon's F12 media (Mediatech) supplemented with 5% fetal bovine serum, vitamins, L-glutamine, penicillin/streptomycin, and 250 µg/ml G418 (Gibco). The cells were washed twice with a sterile phosphate-buffered saline solution and incubated with serum-free DMEM/Coon's F12 media containing 1 mCi of Tran-<sup>35</sup>S-label (ICN) per T75 flask of cells for 5 days at 37°C in a humidified 5% CO<sub>2</sub> atmosphere. The media were harvested, cooled to 4°C, and adjusted to 0.5 M NaCl. The media were loaded onto a 2 ml phenyl-Sepharose (Pharmacia) column pre-equilibrated with 5 mM sodium phosphate, 0.5 M NaCl, pH 7.4. The column was washed with 30 ml of equilibrium buffer, and LCAT was eluted with seven 8-ml fractions of water. Each fraction was recirculated through

the column for 10 min before elution. Fractions 2–7 were pooled and adjusted to 4 mM sodium phosphate, pH 6.9. The phenyl-Sepharose pool was passed through a 2-ml hydroxylapatite (Bio-Rad) column that was washed with 20 ml of 4 mM sodium phosphate, pH 6.9. The flow through and wash were adjusted to 10% glycerol and concentrated with an Amicon pressure concentrator. The purified enzyme was stored in small aliquots at –70°C.

### <sup>35</sup>S-labeled LCAT characterization

Enzyme purity was examined by silver-stained SDS-polyacrylamide gels (SDS-PAGE) as previously published (16) and by autoradiography of dried SDS-polyacrylamide gels. Enzyme activity was measured using rHDL as previously published (16). Enzyme specific activity ranged from 10.3 to 48.2 nmol cholesteryl ester formed/h per µg LCAT. Enzyme mass was quantitated with enzyme-linked immunoassays as previously published and ranged from 15 to 40 µg/ml (16). The purified LCAT was radiolabeled to specific activities of 50,000–260,000 dpm/µg.

### ApoA-I purification and iodination

Human plasma apoA-I was isolated from human HDL by size exclusion chromatography as described previously (17) except that Sephacryl S-200 (Pharmacia) was used as the gel matrix, and the column flow rate was 40 ml/h. ApoA-I was radiolabeled with carrier-free sodium iodide and Iodobeads (Pierce, Rockford, IL), according to the manufacturer's procedures. The radiolabeled apoA-I was diluted to a specific activity of 200,000 dpm/µg with unlabeled apoA-I. The purity of the apoA-I was determined by SDS-PAGE (18).

### Vesicle synthesis

Vesicles were synthesized by mixing 5.6 mg of each phospholipid with trace amounts of [<sup>3</sup>H]cholesterol (1 µCi, New England Nuclear). For vesicles containing *sn*-1 palmitoyl, *sn*-2 arachidonoyl PC (PAPC), *sn*-1 palmitoyl, *sn*-2 docosahexaenoyl PC (PDPC), and *sn*-1 palmitoyl, *sn*-2 eicosapentaenoyl PC (PEPC), phospholipids were synthesized from arachidonic acid, docosahexaenoic acid, and eicosapentaenoic acid and lysolecithin (Sigma) as previously described (7). The phospholipids were dried under nitrogen at room temperature and lyophilized for 30 min. For cholesterol-containing vesicles, *sn*-1 palmitoyl, *sn*-2 oleoyl PC (POPC) and cholesterol were mixed at a 100:20 PC:cholesterol mole ratio with 1 µCi of [<sup>3</sup>H]cholesterol added and dried under nitrogen. The lipids were resuspended in 2 ml of 10 mM Tris, pH 7.4, 0.01% sodium azide, 0.01% ethylenediamine tetraacetic acid (EDTA). The suspension was placed in an ice bath and sonicated continuously for 20 min at 20–50 watts under a nitrogen atmosphere. The

vesicles were purified on a Sepharose CL-4B column (1.75 × 25 cm) using the [<sup>3</sup>H]cholesterol radiolabel to trace the elution profile. Total recovery of [<sup>3</sup>H]cholesterol from the column ranged from 90 to 100%. Fractions containing the tail of the included peak were pooled and concentrated using an Amicon pressure concentrator. The vesicles were stored at 4°C under an argon atmosphere and were used within 4 weeks of preparation. The phospholipid concentration of the vesicles was determined by phospholipid analysis as previously published (19).

#### ApoA-I binding to vesicles

Each binding reaction contained: 5 µg phospholipid, 10 mM Tris, pH 7.4, 0.01% sodium azide, 0.01% EDTA, 800 µg/ml bovine serum albumin (BSA). ApoA-I was added in amounts ranging from 50 to 500 ng (0.0018–0.0179 nmol). The final volume of each reaction was brought to 25 µl with water. The binding reaction was incubated for 15 min at room temperature, which, based on preliminary studies, was long enough for the binding to reach equilibrium. The samples were adjusted to 10% sucrose and 0.01% bromophenol blue and loaded onto a native polyacrylamide gel. Each concentration was performed in triplicate.

#### LCAT binding to vesicles

Each binding reaction contained: 5 µg phospholipid, 10 mM Tris, pH 7.4, 0.01% sodium azide, 0.01% EDTA, 800 µg/ml BSA. LCAT was added in amounts ranging from 100 to 625 ng (0.0015–0.0093 nmol). The final volume of each reaction was brought to 25 µl with water. Based on preliminary studies, the binding reactions were incubated on ice for 1 h in order to reach equilibrium, then adjusted to 10% sucrose and 0.01% bromophenol blue and loaded onto a native polyacrylamide gel. Each reaction concentration was performed in triplicate.

#### LCAT binding to vesicles with prebound apoA-I

ApoA-I was added to vesicles in a 1000:1 phospholipid:apoA-I mole ratio, a subsaturating amount of apoA-I (see Results). The apoA-I and vesicles were preincubated for 15 min at room temperature to allow the apoA-I binding to reach equilibrium. LCAT binding to this mixture was assayed as described above.

#### Native gel electrophoresis

Native polyacrylamide gels were used to separate free protein from vesicle-bound protein based on a modification of methods published by Maurer (20). The running gel consisted of: 6% polyacrylamide (37:1 acrylamide:bisacrylamide ratio, Sigma Chemical Co., St. Louis, MO), 70 mM Tris, pH 7.5, 800 µg/ml BSA. The

stacking gel consisted of: 4% polyacrylamide (37:1 acrylamide:bisacrylamide ratio), 50 mM Tris-phosphate, pH 5.5, and 800 µg/ml BSA. After polymerization, the gels were cooled to 4°C, and cold running buffer was added. The running buffer consisted of: 8 mM Tris-base and 30 mM N-(2-hydroxyethyl)piperazine-N'-2-ethanesulfonic acid (HEPES), pH 7.4. The 8 × 10 cm gels were run at 25 mA/gel for 30 min at 4°C, transferred to filter paper, and dried under a vacuum.

#### Quantitation of binding

The dried gels were exposed to a Molecular Dynamics phosphorimager cassette overnight. The phosphorimager scans the exposed cassette and converts the amount of luminescence detected to a volume measurement. This measurement is directly proportional to the amount of radioactive decay the screen was exposed to. After scanning the phosphorimage screen, the volume representing the total radioactivity (total protein) in each lane and the volume representing the amount of radioactivity in the top 1/3 of each lane (bound protein) was quantitated using the Molecular Dynamics Imagequant program. Empty lanes were used to determine the volume that represented background radioactivity for the total and bound fractions. This background was subtracted from each measurement. A specific activity for the radiolabeled protein was calculated by dividing the mean of the total volume in each lane by the amount of labeled protein loaded onto the lanes (volume/nmole). The mean of the six different concentrations was used as the specific activity of the protein. The standard deviation of these values was less than 10% in each experiment. The volume representing free protein was calculated by subtracting the volume of the bound protein from the volume of the total protein. The volume measurements for each protein concentration were converted to nmoles of protein by dividing the means of the total, bound, and free protein of each triplicate sample by the calculated specific activity. The dissociation constant ( $K_d$ ) and binding capacity ( $B_{max}$ ) were determined using a Scatchard analysis (21).

#### Data analysis

Data are reported as mean ± standard error of the mean (SEM) or standard deviation. Analysis of variance and Fisher's least significant difference test were used for statistical analysis of the data.

## RESULTS

In order to study LCAT interfacial binding, <sup>35</sup>S-labeled LCAT (<sup>35</sup>S-LCAT) was produced using a stably

transfected CHO expression system containing Tran-<sup>35</sup>S-Label, a mixture of radiolabeled methionine and cysteine. After 5 days of incubation, the media were harvested, and <sup>35</sup>S-LCAT was purified using phenyl-Sepharose and hydroxylapatite column chromatography (16). SDS-PAGE was used to analyze the purity of the enzyme after the final step (Fig. 1). Enzyme purity ranged from 80 to 95% pure based on radioactivity distribution. This method of LCAT purification and labeling was used for all subsequent experiments.

To measure binding affinities and capacities, vesicle-bound LCAT was separated from unbound LCAT using a native gel electrophoresis system developed from procedures published by Maurer (20). The gel system was chosen to minimize changes in experimental conditions between the binding incubation step and the gel separation step. The Tris-HEPES gel buffers resulted in the gel running at pH 7.0 in the stacker and pH 8.0 in the separating gel. The 4% polyacrylamide stacking gel separated the free protein from the vesicles in less than 30 min at 4°C. Figure 2 is a phosphorimage of a control gel demonstrating that under all conditions the vesicles migrated only into the top third of the stacking gel. Even in the presence of both LCAT and apoA-I (lane 4), the migration characteristics of the vesicle were unchanged compared to vesicle alone (lane 1). Unbound <sup>35</sup>S-LCAT (lane 6) and unbound <sup>125</sup>I-labeled apoA-I (lane 5) ran with the dye front, resulting in a quick separation of unbound protein from the vesicle.

In order to demonstrate the effectiveness of native gel electrophoresis, apoA-I binding to POPC vesicles with cholesterol was measured (Fig. 3) and compared to published values. In the gel (Fig. 3A), the iodinated apoA-I migrated as two bands; the top band coincided

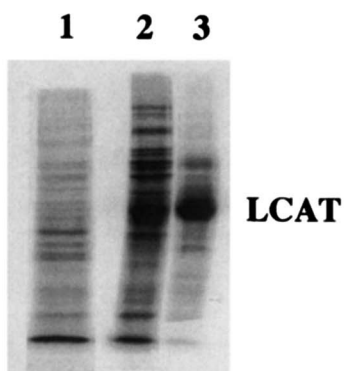


**Fig. 1.** Phosphorimage of SDS-PAGE of <sup>35</sup>S-labeled LCAT purification. SDS-polyacrylamide gel electrophoresis was used to check the purity of the enzyme preparations. After electrophoresis, the gels were silver stained, dried, and exposed overnight in a Molecular Dynamics phosphorimager cassette. Lane 1, starting media; lane 2, the phenyl-Sepharose concentrated pool; lane 3, the concentrated hydroxylapatite flow through.

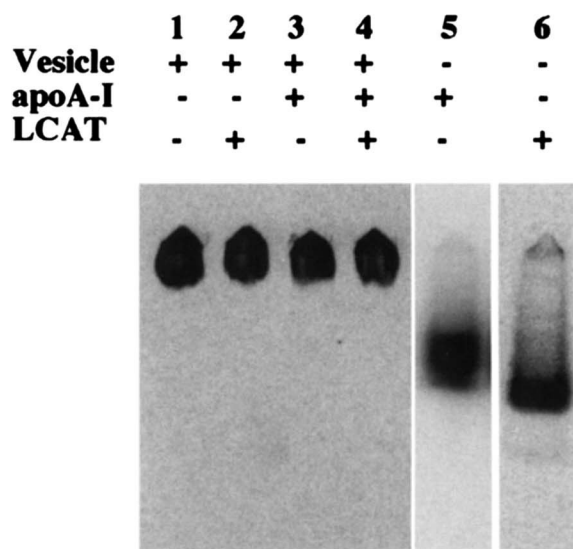


**Fig. 2.** Phosphorimager analysis of the mobility of POPC vesicles, free LCAT, and apoA-I. The POPC vesicles (5 µg) containing trace amounts of [<sup>14</sup>C]cholesterol were incubated with LCAT (625 ng) and apoA-I (500 ng) as described in Methods. Native gel electrophoresis followed by phosphorimage analysis were used to determine the migration of: lane 1, <sup>3</sup>H-labeled vesicles alone; lane 2, <sup>3</sup>H-labeled vesicles + unlabeled LCAT; lane 3, <sup>3</sup>H-labeled vesicles + unlabeled apoA-I; lane 4, <sup>3</sup>H-labeled vesicles + unlabeled LCAT + unlabeled apoA-I; lane 5, <sup>125</sup>I-labeled apoA-I, and lane 6, <sup>35</sup>S-labeled LCAT.

with the position of the vesicles (bound), and the bottom band coincided with unbound apoA-I (free). The amount of radioactivity was converted into nmoles apoA-I bound and plotted in the corresponding binding curve (Fig. 3B). Scatchard analysis (Fig. 3C) was used to calculate the binding affinity ( $K_d$ ) and binding capacity ( $B_{max}$ ) of apoA-I for the POPC vesicles. Under these conditions, a  $K_d$  of 700 nM was calculated with a  $B_{max}$  of 1.6 moles apoA-I bound/1000 moles of POPC.

The binding of apoA-I was further characterized using phospholipids that contained long chain, PUFA in the *sn*-2 position. As can be seen in Fig. 4, the binding of apoA-I to PEPC, PAPC, and PDPC approaches saturation at lower apoA-I concentrations than apoA-I binding to POPC. In all cases, the amount of protein bound was decreased in the presence of the polyunsaturated phospholipids. Table 1 compares the binding affinities and capacities determined from these analyses. ApoA-I binding to POPC with and without cholesterol demonstrated no detectable difference in binding, thus combining the data results in an overall  $K_d$  of 731 nM and a  $B_{max}$  of 1.47 apoA-I/1000 PC. The apoA-I dissociation constants for PAPC, PEPC, and PDPC are 4- to 10-fold less than that of apoA-I binding to POPC. In all cases the  $B_{max}$  is also significantly reduced from 1.47 apoA-I/1000 PC with POPC to less than 0.3 apoA-I/1000 PC for PAPC, PEPC, and PDPC.

## 3A

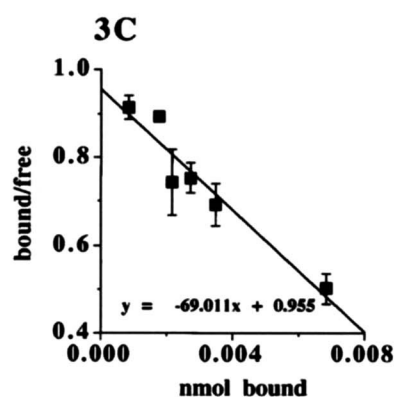
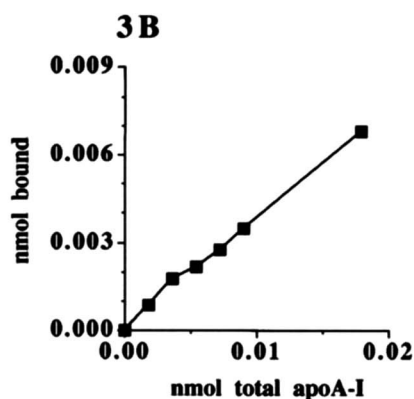
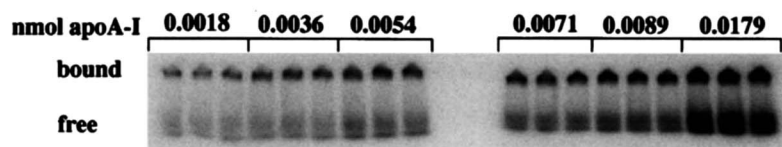


**Fig. 3.** A representative experiment of apoA-I binding to POPC vesicles containing 14 mole % cholesterol. Increasing amounts of apoA-I were incubated with 5  $\mu$ g of phospholipid vesicles for 15 min at room temperature. These reactions were loaded onto a native polyacrylamide gel and electrophoresed for 30 min at 4°C. The gels were dried and exposed on the phosphorimager (Fig. 3A). The total and bound radioactivity were quantitated and used to calculate free apoA-I. Figure 3B is a binding plot from these data. Scatchard analysis (Fig. 3C) was used to determine  $K_d$  and  $B_{max}$  (mean  $\pm$  standard deviation of triplicate measurements).

The binding of LCAT to POPC, PAPC, PEPC, and PDPC was measured under conditions similar to the binding of apoA-I. **Figure 5** is a sample data set of LCAT binding to 100% POPC vesicles. **Figure 5A** is the phosphorimage of the native gel and demonstrates that LCAT also runs as two bands in the presence of vesicles. The upper band comigrates with the vesicles and corre-

sponds to the bound LCAT, whereas the lower band comigrates with unbound LCAT. In this case, the binding curve (**Fig. 5B**) shows that the binding is approaching saturation. The Scatchard plot (**Fig. 5C**) was used to calculate the  $K_d$  and  $B_{max}$  of the experiment.

The influence of cholesterol on LCAT binding was examined by measuring the binding affinities and capacities in the presence of 0 mole % and 14 mole % cholesterol in POPC vesicles. **Figure 6** shows the binding data; **Table 2** summarizes the binding affinities and capacities. The dissociation constant in the presence of 14 mole % cholesterol decreases from 2190 nM to 530

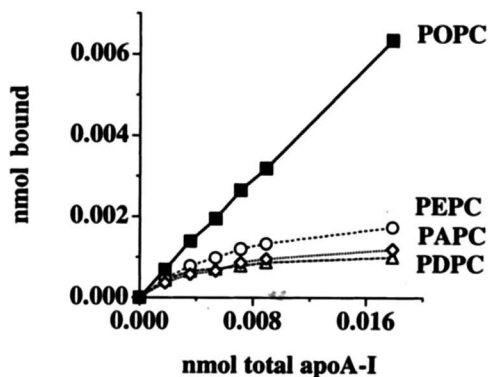


**Fig. 4.** ApoA-I binding to POPC, PEPC, PAPC, and PDPC. Binding reactions as described in Methods were used to measure apoA-I binding to different phospholipids. The data in the binding plots are the mean of 3–8 binding experiments for POPC ( $n = 8$ ), PAPC ( $n = 3$ ), PEPC ( $n = 3$ ), and PDPC ( $n = 3$ ).

**TABLE 1.** Binding constants for ApoA-I to vesicles

Vesicle PC	n	$K_d$	$B_{max}$
		nM	apoA-I molecules/1000 PC
POPC	6	$747 \pm 84$	$1.4 \pm 0.1$
POPC + 14 mol % chol.	2	696	1.6
PAPC	3	$177 \pm 11^a$	$0.2 \pm 0.01^a$
PEPC	3	$151 \pm 17^a$	$0.3 \pm 0.05^a$
PDPC	3	$75 \pm 18^a$	$0.1 \pm 0.01^a$

Values given as mean  $\pm$  SEM. Binding constants were derived from Scatchard analysis of the binding curves shown in **Fig. 4**; n, number of independent experiments.

<sup>a</sup>Significantly different from POPC by analysis of variance and Fisher's least significant difference test ( $P < 0.0001$ ).

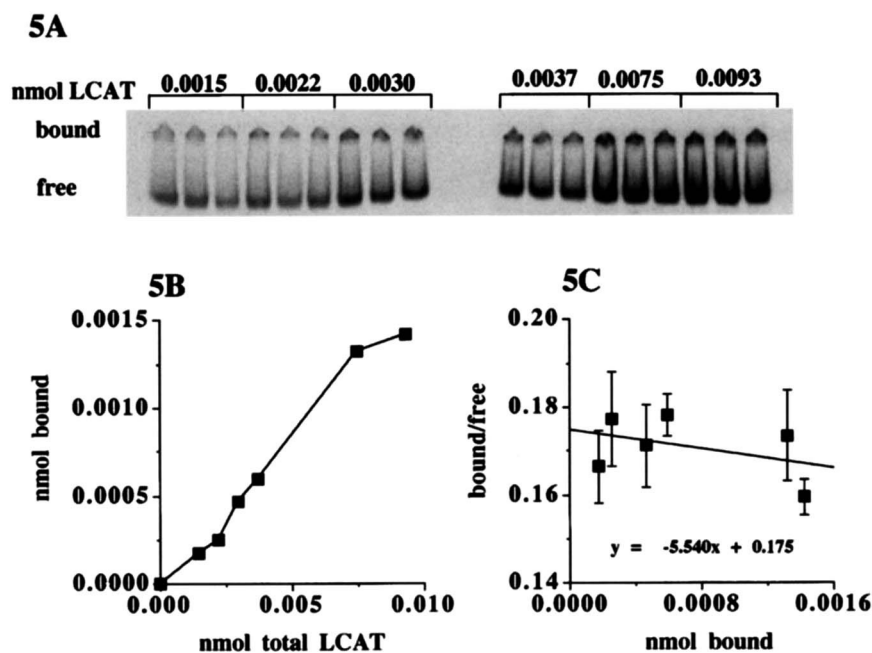


**Fig. 5.** LCAT binding to POPC. Increasing quantities of LCAT were bound to 5  $\mu$ g phospholipid and separated by native polyacrylamide gel electrophoresis (top panel). LCAT incubations were done at 4°C for 1 h before loading the gel. The binding curve for this experiment is shown in Fig. 5B. A Scatchard plot (Fig. 5C) was used to determine binding affinity and capacity. Values are the mean  $\pm$  the standard deviation of triplicate measurements.

nM, while the  $B_{max}$  decreases from 2.6 LCAT/1000 PC to 0.6 LCAT/1000 PC. The influence of apoA-I on the binding of LCAT to 100% POPC vesicles and to 100:17 mole % POPC: cholesterol vesicles was also examined. The dissociation constant was not significantly reduced in the presence of apoA-I (2190 nM to 944 nM) nor was the  $B_{max}$  decreased significantly (2.63 LCAT/

1000 PC to 1.1 LCAT/1000 PC; Table 2). However, the dissociation constant and  $B_{max}$  for LCAT binding were both significantly less for POPC vesicles containing cholesterol compared to cholesterol-free POPC vesicles regardless of whether apoA-I was present or absent in the incubation mixture.

The influence on LCAT interfacial binding of phospholipids containing long chain, PUFAs in the *sn*-2 position was characterized in a similar manner (Fig. 7). LCAT binding to PDPC was undetectable by this method of analysis. LCAT binding to PAPC vesicles demonstrated a reduced dissociation constant and binding capacity (611 nM and 0.7 LCAT/1000 PC, respectively) compared to that of POPC vesicles (Table 2). However, the binding of LCAT to PEPC was indistinguishable from LCAT binding to POPC.

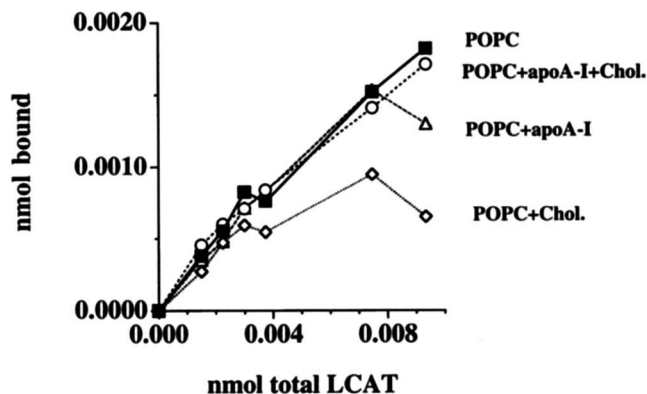


**Fig. 6.** Binding curves of LCAT binding to POPC, POPC preincubated with apoA-I, POPC with 14 mole % cholesterol and POPC with 17 mole % cholesterol preincubated with apoA-I. The binding plots were determined as described in Methods and are the mean of at least three experiments for POPC (n = 4), POPC preincubated with apoA-I (n = 3), POPC with 14 mole% cholesterol (n = 3), and POPC with 17 mole% cholesterol preincubated with apoA-I (n = 4).

## DISCUSSION

Interfacial binding of LCAT to HDL substrate particles is the first step in cholesteryl ester synthesis. However, little is known regarding the factors that influence the interfacial binding of LCAT. Factors could include HDL PC fatty acyl composition and surface cholesterol and apoA-I content. The purpose of this study was to

TABLE 2. Binding constants of LCAT to vesicles

Vesicle Preparation	n	$K_d$	$P$ Value <sup>a</sup>	$B_{max}$	$P$ Value
		nm		LCAT molecules/1000 PC	
POPC	4	2190 ± 640	—	2.6 ± 0.86	—
POPC + apoA-I	3	944 ± 203	NS	1.1 ± 0.07	NS
POPC + 14 mol% chol.	3	530 ± 260	0.008	0.6 ± 0.06	0.003
POPC + 17 mol% chol + apoA-I	4	421 ± 103	0.005	0.7 ± 0.1	0.002
PAPC	4	611 ± 332	0.03	0.7 ± 0.3	0.03
PEPC	3	2041 ± 823	NS	2.5 ± 1.2	NS

Values given as mean ± SEM. Binding constants were derived from Scatchard analysis of the binding curves shown in Figs. 6 and 7; n, number of independent experiments.

<sup>a</sup> $P$  value compared to POPC, determined by analysis of variance and Fisher's least significant difference test; NS, not significant at  $P = 0.05$ .

explore the influence of these factors on LCAT interfacial binding using small unilamellar vesicles as a model system for the HDL interface. Vesicles were used because their size distribution and lipid composition can be well controlled. Using human LCAT that was metabolically radiolabeled and enzymatically active, we demonstrated that vesicle PC fatty acyl composition and cholesterol content have a significant influence on LCAT binding to vesicles, decreasing both the dissociation constant and the number of LCAT molecules bound at saturation, whereas apoA-I appeared to have minimal effect. These data suggest that the lipid composition of the lipoprotein particle may influence LCAT activity through effects on interfacial binding.

Quantitation of LCAT and apoA-I interfacial binding was performed using native gel electrophoresis to separate vesicle-bound protein from unbound protein. As the binding characteristics of apoA-I have been studied previously, apoA-I binding was examined in order to demonstrate the validity of this technique. Using gel filtration, Yokoyama et al. (14) found that apoA-I binding

to egg yolk lecithin vesicles had a decreased  $K_d$  with increased cholesterol (900 nM at 0 mole % cholesterol to 300 nM at 20 mole %) but also found an increased binding capacity with increased cholesterol (1.74 apoA-I/1000 PC at 0 mole % cholesterol and 3.7 apoA-I/1000 PC at 20 mole %). Derksen and Small (15) examined apoA-I binding to egg yolk lecithin, triolein, and cholesterol emulsions by gradient centrifugation to separate lipid-bound protein from unbound protein. With this substrate, apoA-I binding affinity was unaffected by cholesterol concentration ( $K_d = 740$ -810 nM); however, the binding capacity decreased with increased cholesterol (3.8 apoA-I/1000 PC at 7.8% wt/wt cholesterol to 0.6 apoA-I/1000 PC at 32.6% wt/wt cholesterol). In our study, native gel electrophoresis was used to measure apoA-I binding to POPC vesicles, and a  $K_d$  of  $731 \pm 65$  nM and a binding capacity of  $1.5 \pm 0.1$  apoA-I/1000 PC were measured. No influence of cholesterol on either  $K_d$  or binding capacity was observed. Thus, our values are similar to those of Yokoyama et al. (14) and Derksen and Small (15), indicating that native gel electrophoresis can be used to quantify protein binding to vesicles.

Although the lipid binding of apoA-I has been extensively studied, no comparison of binding to different PC species with varying fatty acyl composition has been performed with vesicles. Thus, we examined the binding of apoA-I to phospholipids containing long chain polyunsaturated fatty acyl chains in the *sn*-2 position. We found that apoA-I bound with higher affinity but lower capacity to PAPC, PDPC, and PEPC when compared to POPC. Parks and Thuren (13) measured apoA-I binding to phospholipid monolayers composed of POPC, PEPC, and PDPC. The authors concluded that PEPC and PDPC bound apoA-I with a decreased affinity but a capacity similar to that of POPC. However, the measured affinities were 350- to 700-fold tighter than those measured in this and other studies (14, 15). The tighter binding may be an inherent property of the monolayer system. It is possible that phospholipids in a monolayer may increase protein binding affinities due

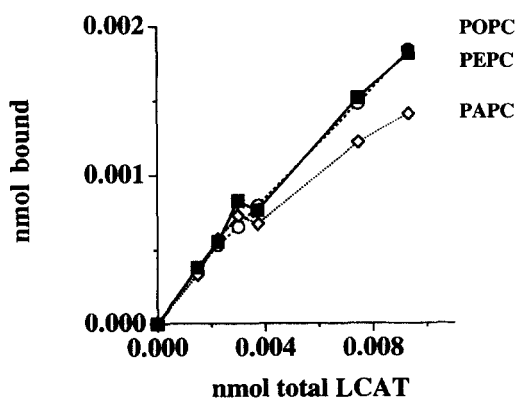


Fig. 7. LCAT binding to POPC, PAPC, and PEPC. Binding curves for LCAT binding to POPC (n = 4), PAPC (n = 4), and PEPC (n = 3) were performed as described in Methods.

to the organization of the phospholipid surface or to differences in the lateral surface pressure between planar and spherical phospholipid surfaces. If one assumes a plasma apoA-I concentration of 120 mg/dl or 43  $\mu\text{M}$  (22), the plasma concentration is approximately 50-fold greater than the  $K_d$  for apoA-I binding to vesicles. Therefore, it is reasonable to assume that apoA-I binding to the HDL surface is dominated by factors that affect the maximum binding capacity, such as the fatty acyl composition of the PC species as observed in this study.

The interfacial binding of LCAT was characterized by comparing binding to POPC vesicles with different cholesterol concentrations, and in the presence or absence of apoA-I. The association of cholesterol with POPC vesicles increased LCAT binding affinity but decreased LCAT binding capacity. Although similar trends were observed for LCAT binding in the presence of POPC vesicles and apoA-I, the difference did not reach statistical significance. The increased  $K_d$  observed with cholesterol-containing POPC vesicles may be the result of a more productive binding conformation or a more specific interaction with the phospholipid surface due to altered phospholipid organization caused by the cholesterol. The decrease in capacity may also indicate that a different binding complex is formed in the presence of the substrate cholesterol, perhaps due to the condensing effect of cholesterol on phospholipid bilayers (23).

There have been several published studies on LCAT interfacial binding. Bolin and Jonas (10) measured LCAT binding to recombinant HDL disks composed of egg yolk lecithin and cholesterol. The dissociation constants ranged from 17 to 27  $\mu\text{M}$  PC depending on the method of measurement. In another study the LCAT dissociation constant was found to increase from 23  $\mu\text{M}$  PC to 69  $\mu\text{M}$  PC with increasing rHDL sphingomyelin content (11). It is difficult to directly compare the values in our study with those of Bolin and Jonas (10), as their dissociation constants were given in terms of apoA-I or PC concentration rather than LCAT concentration. Other methodological differences exist among the studies including the type of substrate particle used and the method of radiolabeling LCAT. However, graphical estimation of  $K_d$  based on LCAT concentration (ref. 10, Fig. 2) gave a value of 300 nM, which is in the range of values obtained in this study with cholesterol containing vesicles (Table 2). Weinberg et al. (12) also measured LCAT binding to egg yolk lecithin monolayers. The 1.5 nM LCAT dissociation constant is significantly lower than that measured in our study with POPC vesicles (2190 nM LCAT). This difference may be an inherent function of measuring binding to a planar lipid monolayer as discussed above for apoA-I.

rHDL containing PC with long chain PUFA in the *sn*-

2 position have a decreased reactivity to LCAT compared to rHDL containing POPC (6–9). A reasonable hypothesis to explain this observation is a decrease in interfacial binding of LCAT to the rHDL containing long chain PUFA. However, our data do not support this hypothesis, at least with regard to LCAT binding to vesicles, as the binding to PEPC vesicles was the same as POPC vesicles, whereas the PAPC vesicles had a significantly decreased  $K_d$  and maximum binding capacity (Table 2). However, the LCAT reactivities of PEPC and PAPC rHDL with human LCAT are nearly identical (6, 7). Furthermore, the apparent  $K_m$  of the LCAT reaction, which has been suggested to reflect predominantly the interfacial binding preference of LCAT (10), was found to be similar for rHDL containing PEPC and PAPC (6). Taken together, these results suggest that differences in interfacial binding of LCAT do not adequately explain the differences in LCAT reactivity among rHDL containing PUFA species. A more likely explanation is that the differences in reactivity are the result of a decreased interaction of PC species containing PUFA at the active site of the enzyme, which would be reflected in the  $\text{app}V_{\text{max}}$  for the enzyme reaction (10). In support of this explanation is the 2- to 10-fold variation in apparent  $V_{\text{max}}$  among rHDL containing PUFA compared to POPC (6).

Two models for LCAT binding to nascent HDL or rHDL have been proposed. In the first model, LCAT is envisioned to bind first to the phospholipid surface on the face of the discoidal particle and translocate to the edge, where it becomes activated by apoA-I or binds phospholipid and cholesterol that has been activated by apoA-I (24). Another model suggests that a region of LCAT primary sequence (amino acids 151–174) that is amphipathic and resembles a lipid binding region of apolipoprotein E (amino acids 268–288) displaces an amphipathic helix of apoA-I on the edge of the discoidal HDL particle (2). The binding of this region of LCAT is stabilized and the enzyme is activated by its charge–charge interaction with apoA-I. While our LCAT binding data cannot distinguish between either of these two models, we favor the former as our data do suggest that cholesterol content of the substrate particle surface may have a bigger impact on LCAT binding than apoA-I, at least under our experimental conditions. ■■

This work was supported by grants from the National Heart, Lung, and Blood Institute of the National Institutes of Health (HL49373 and HL54176), and by a fellowship (K. R. M.) from the North Carolina affiliate of the American Heart Association (NC-94-FW-07). The authors gratefully acknowledge the technical assistance of Kevin Huggins and the editorial assistance of Karen Klein.

Manuscript received 22 August 1996 and in revised form 19 February 1997.



## REFERENCES

- Fielding, C. J. 1990. Lecithin:cholesterol acyltransferase. In *Advances in Cholesterol Research*. M. Esfahani and J. B. Swaney, editors. Telford Press, Caldwell, NJ. 271–314.
- Fielding, C. J., and P. E. Fielding. 1995. Molecular physiology of reverse cholesterol transport. *J. Lipid Res.* **36**: 211–228.
- Hide, F. K., L. Chan, and W. Li. 1992. Structure and evolution of the lipase superfamily. *J. Lipid Res.* **33**: 167–178.
- Winkler, F. K., A. D'Arcy, and W. Hunziker. 1990. Structure of human pancreatic lipase. *Nature*. **343**: 771–774.
- Dugi, K. A., H. L. Dichek, G. D. Talley, H. B. Brewer, Jr., and S. Santamarina-Fojo. 1992. Human lipoprotein lipase: the loop covering the catalytic site is essential for interaction with lipid substrates. *J. Biol. Chem.* **267**: 25086–25091.
- Parks, J. S., and A. K. Gebre. 1997. Long-chain polyunsaturated fatty acids in the *sn*-2 position of phosphatidylcholine decrease the stability of recombinant high density lipoprotein apolipoprotein A-I and the activation energy of the lecithin:cholesterol acyltransferase reaction. *J. Lipid Res.* **38**: 266–275.
- Parks, J. S., T. Y. Thuren, and J. D. Schmitt. 1992. Inhibition of lecithin:cholesterol acyltransferase activity by synthetic phosphatidylcholine species containing eicosapentaenoic acid or docosahexaenoic acid in the *sn*-2 position. *J. Lipid Res.* **33**: 879–887.
- Jonas, A., N. L. Zorich, K. E. Kezdy, and W. E. Trick. 1987. Reaction of discoidal complexes of apolipoprotein A-I and various phosphatidylcholines with lecithin:cholesterol acyltransferase. Interfacial effects. *J. Biol. Chem.* **262**: 3969–3974.
- Parks, J. S., B. C. Bullock, and L. L. Rudel. 1989. The reactivity of plasma phospholipids with lecithin:cholesterol acyltransferase is decreased in fish oil-fed monkeys. *J. Biol. Chem.* **264**: 2545–2551.
- Bolin, D. J., and A. Jonas. 1994. Binding of lecithin:cholesterol acyltransferase to reconstituted high density lipoproteins is affected by their lipid but not apolipoprotein composition. *J. Biol. Chem.* **269**: 7429–7434.
- Bolin, D. J., and A. Jonas. 1996. Sphingomyelin inhibits the lecithin-cholesterol acyltransferase reaction with reconstituted high density lipoproteins by decreasing enzyme binding. *J. Biol. Chem.* **271**: 19152–19158.
- Weinberg, R. B., J. B. Jones, P. H. Pritchard, and A. G. Lacko. 1995. Effect of interfacial pressure on the binding and phospholipase A<sub>2</sub> activity of recombinant human lecithin-cholesterol acyltransferase. *Biochem. Biophys. Res. Commun.* **211**: 840–846.
- Parks, J. S., and T. Y. Thuren. 1993. Decreased binding of apoA-I to phosphatidylcholine (PC) monolayers containing 22:6 n-3 in the *sn*-2 position. *J. Lipid Res.* **34**: 779–788.
- Yokoyama, S., D. Fukushima, J. P. Kupferberg, F. J. Kezdy, and E. T. Kaiser. 1980. The mechanism of activation of lecithin:cholesterol acyltransferase by apolipoprotein A-I and an amphiphilic peptide. *J. Biol. Chem.* **255**: 7333–7339.
- Derksen, A., and D. M. Small. 1989. Interaction of apoA-I and apoE-3 with triglyceride-phospholipid emulsions containing increasing cholesterol concentrations. Model of triglyceride-rich nascent and remnant lipoproteins. *Biochemistry*. **28**: 900–906.
- Miller, K. R., J. Wang, M. Sorci-Thomas, R. A. Anderson, and J. S. Parks. 1996. Glycosylation structure and enzyme activity of lecithin:cholesterol acyltransferase from human plasma, HepG2 cells, and baculoviral and Chinese hamster ovary cell expression systems. *J. Lipid Res.* **37**: 551–561.
- Parks, J. S., and L. L. Rudel. 1979. Isolation and characterization of high density lipoprotein apoproteins in the non-human primate (vervet). *J. Biol. Chem.* **254**: 6716–6723.
- Laemmli, U. K. 1970. Cleavage of structural proteins during the assembly of the head of bacteriophage T4. *Nature*. **227**: 680–685.
- Fiske, C. H., and Y. SubbaRow. 1925. Colorimetric determination of phosphorus. *J. Biol. Chem.* **66**: 357–400.
- Maurer, H. R. 1971. *Disc Electrophoresis and Related Techniques of Polyacrylamide Gel Electrophoresis*. Walter de Gruyter, Berlin. 43–52.
- Scatchard, G. 1949. The attractions of proteins for small molecules and ions. *Ann. NY Acad. Sci.* **51**: 660–672.
- Mahley, R. W., T. L. Innerarity, S. C. Rall, Jr., and K. H. Weisgraber. 1984. Plasma lipoproteins: apolipoprotein structure and function. *J. Lipid Res.* **25**: 1277–1294.
- Schroeder, F., J. R. Jefferson, A. B. Kier, J. Knittel, T. J. Scallen, W. G. Wood, and I. Hapala. 1991. Membrane cholesterol dynamics: cholesterol domains and kinetic pools. [Review]. *Proc. Soc. Exp. Biol. Med.* **196**: 235–252.
- Jonas, A. 1991. Lecithin-cholesterol acyltransferase in the metabolism of high-density lipoproteins. *Biochim. Biophys. Acta.* **1084**: 205–220.